

# CMOS-compatible SOI Micro-Hotplate-based Oxygen Sensor

Viorel Avramescu<sup>1\*</sup>, Andrea De Luca<sup>2</sup>, Mihai Brezeanu<sup>1</sup>, Syed Zeeshan Ali<sup>3</sup>, Florin Udrea<sup>2,3</sup>, Octavian Buiu<sup>1</sup>, Cornel Cobianu<sup>1</sup>, Bogdan Serban<sup>1</sup>, Julian Gardner<sup>4</sup>, Viorel Dumitru<sup>1</sup>, Alisa Stratulat<sup>1</sup>

<sup>1</sup>Sensors and Wireless Lab Bucharest, ACS Global Lab, Honeywell Romania, 169A Calea Floreasca, Bucharest

<sup>2</sup>University of Cambridge, Department of Engineering, CAPE Building, 9 JJ Thomson Avenue, Cambridge CB3 0FA, UK

<sup>3</sup>Cambridge CMOS Sensors Ltd, Deanland House, 160 Cowley Road, Cambridge CB4 0DL, UK

<sup>4</sup>University of Warwick, School of Engineering, Coventry CV4 7AL, UK

[viorel.avramescu@honeywell.com](mailto:viorel.avramescu@honeywell.com)

**Abstract** — The paper reports upon the design and characterization of a resistive O<sub>2</sub> sensor, which is fully CMOS-compatible and is based on an ultra-low-power Silicon on Insulator (SOI) micro-hotplate membrane. The microsensor employs SrTi<sub>0.4</sub>Fe<sub>0.6</sub>O<sub>2.8</sub> (STFO60) as sensing layer. Thermo-Gravimetric Analysis (TGA) Energy-Dispersive X-ray Spectroscopy (EDX), X-ray Diffraction (XRD) and Scanning Electron Microscope (SEM) techniques have been used to assess the quality of both the sensing layer and STFO-SOI interface. At room temperature, the SOI sensor shows good sensitivity and fast response time ( $\leq 6$  seconds) to O<sub>2</sub> concentration ranging from 0% to 20% in a nitrogen atmosphere. This is the first experimental result showing the potential of this structure as O<sub>2</sub> sensor.

## I. INTRODUCTION

Industrial applications, such as combustion optimization and emission monitoring in automotive, as well as domestic and other small-scale boilers, require low cost, low power, and fast O<sub>2</sub> sensors. They should be capable of reliable operation both at room temperature and in harsh environment conditions (temperatures up to 225°C, high levels of relative humidity up to 100%, condensing environments). The sensors currently available on the market fail to fulfill one or more of these requirements. For example, optical technologies have either serious reliability issues, especially when used above room temperature, or are expensive and suitable mainly for applications such as industrial boilers and power plants [1]. Oxygen-pump electrochemical oxygen sensors employing Ytria Stabilized Zirconia (YSZ) are expensive, have very high power consumption and require a reference chamber filled with clear air [2]. Solutions which do not require fresh air as reference have been also proposed [3], but, due to the complexity of the technological process, they lack the opportunity of large-scale production, which puts a serious limitation on lowering the final cost of the sensor. Finally, oxygen paramagnetic sensors are far too expensive for most domestic and industrial applications.

It is the purpose of this paper to introduce a resistive O<sub>2</sub> sensor employing STFO60 as sensing layer on an SOI micro-

hotplate membrane, employing a heater made of doped single crystal silicon. The technology is fully CMOS-compatible, thus potentially yielding highly scalable, low cost sensors. The nature of the silicon (p-type Si) and SiO<sub>2</sub> layers enables stable operation at high temperatures, with the membrane design ensuring extremely low power consumption [4]. At the same time, the suitability of STFO60 as O<sub>2</sub> sensing layer has already been demonstrated in an O<sub>2</sub> probe tested on a diesel engine car under real driving conditions [5]. This study presents the first experimental results obtained after depositing an STFO60 layer on a fully CMOS-compatible SOI micro-hotplate membrane, with Si heater, and measuring its oxygen sensing capability.

## II. SENSOR DESIGN

### A. SOI Membrane

Fig. 1 shows a schematic cross section of the SOI micro-hotplate membrane employed in this study. The SOI membrane was formed by the Deep Reactive Ion Etching (DRIE) of a bulk silicon layer, above which a 5 $\mu$ m thick membrane was fabricated. The membrane comprises layers of high quality buried SiO<sub>2</sub>, silicon and SiO<sub>2</sub>. The silicon die (Fig. 2) was fabricated in a commercial 6" wafer SOI CMOS process. A p-doped single crystal silicon resistive heater was embedded in the SiO<sub>2</sub> membrane. The microheater has a diameter of 300 $\mu$ m and a resistance of 91 $\Omega$ , at ambient temperature. The circular membrane features a diameter of 600 $\mu$ m. Si<sub>3</sub>N<sub>4</sub> was used as passivation layer. Post-CMOS deposited gold interdigitated electrodes (IDEs), with an aspect ratio of 320, allowed electrical contact to the semiconductor sensing layer.

Key advantages of the SOI micro-hotplates employed in this study are the very low DC power consumption and high temperature uniformity across the heater sensing area. The use of a commercial CMOS process means that the devices can be fabricated in high volume (millions), at low unit cost. The p-type single crystal silicon heater is used because it is stable at high temperatures (compared to doped polysilicon, for example, especially above 400°C), and has a closer temperature coefficient of expansion (TCE) to silicon dioxide than metal heaters.

This work has been funded by the EU FP7 SOI-HITS (Smart Silicon-on-Insulator Sensing Systems Operating at High Temperature) project. For more details, see [www.soi-hits.eu](http://www.soi-hits.eu).

Results from Fig. 3 demonstrate the approximately linear relationship between the measured heater temperature and its DC power consumption.

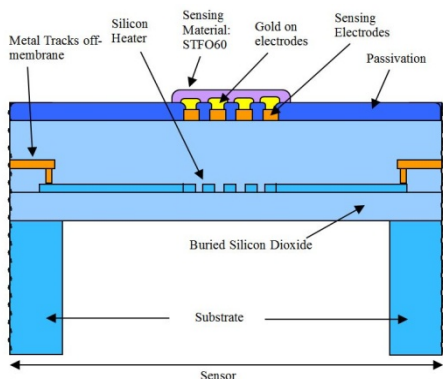


Fig. 1. SOI CMOS micro-hotplate cross-section.

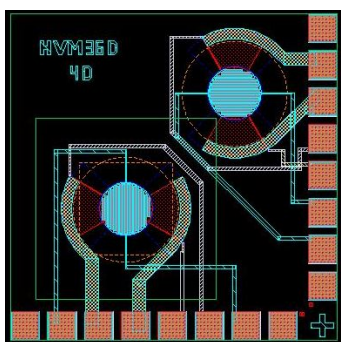


Fig. 2. Layout of dual micro-hotplate chip (2mm x 2mm), used here for testing

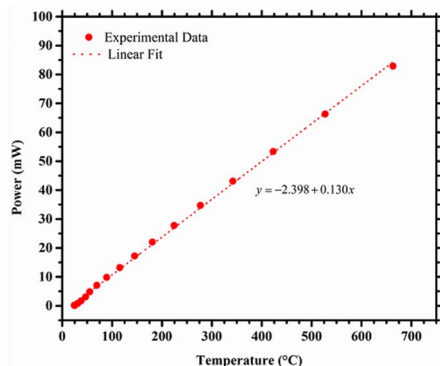


Fig. 3. Measured DC power consumption as function of the heater temperature with linear fit.

The average power consumption can be substantially reduced when the heater is driven in a pulse-mode (~mW). This driving method is possible because of the very small thermal mass of the SOI membrane, which results in a thermal rise time (10% - 90%) of approx. 20ms. Fig. 4 shows a typical, 3D-simulated temperature distribution across a circular SOI micro-hotplate; as expected, the temperature is highest above the heater and decreases almost linearly down to ambient temperature at the edge of the membrane structure. One should note the extremely uniform temperature distribution over the entire sensing area.

Several resistive gas sensors have been demonstrated in the past based upon this type of SOI micro-hotplate. As a sensing

layer, the resistive sensors employed either nanomaterials or thin layer metal oxides grown or deposited on the SOI substrate. For example, zinc-oxide nanowires grown on the SOI micro-hotplate have been used for detecting NO<sub>2</sub>

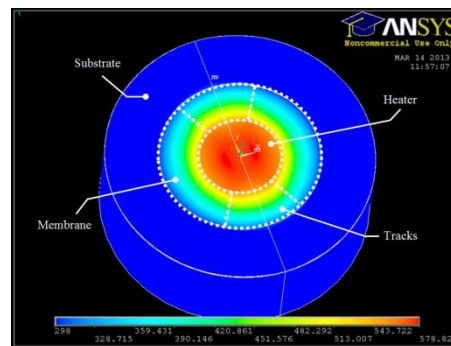


Fig. 4. SOI micro-hotplate temperature profile as predicted by the Finite Element Module of the Ansys simulator

(the minimum detection threshold was sub-ppm concentration [6]), ethanol [7], hydrogen (minimum detection threshold around 100ppm - [8]), and toluene (concentrations above 400ppm- [9]). ‘Spaghetti-like’ carbon nanotubes, also grown on the SOI membrane, have been found to be sensitive to NO<sub>2</sub> (sub-ppm concentration were measured) [10] and methane (500ppm, as minimum detection threshold - [11]). At the same time, deposited tungsten-doped lanthanum iron oxide has shown response to ethanol [12], while deposited tungsten molybdenum oxide was found to be able to detect concentrations of NO<sub>2</sub> as low as 0.1ppm [13].

### B. STFO Sensing Layer

Several types of SrTi<sub>1-x</sub>Fe<sub>x</sub>O<sub>3-δ</sub> (STFO) have been proposed in the literature to be suitable candidates as O<sub>2</sub> resistive sensing layers [14 - 16]. While varying the ratio between the Ti and the Fe concentrations (and keeping their sum constant), it has been found that the temperature coefficient of resistance (TCR) changes from negative to positive values as the Fe concentration increases. For a certain Ti:Fe ratio, STFO shows zero temperature coefficient. Depending on the manufacturing method, STFO exhibits TCR=0 either for 35% Fe and 65% Ti (yielding STFO35, as in [15]), or for 60% Fe and 40% Ti (yielding STFO60, as in [16]). For the latter, the temperature independence of the electrical resistance occurs if the layer is heated to temperatures between 450°C and 650°C. In an experiment meant to prove the suitability of STFO60 as sensing layer for O<sub>2</sub> resistive sensors operating in harsh environment, a 30μm thick STFO60 layer was deposited by screen printing on a 6mm × 3mm alumina substrate [5]. A Pt heater was embedded in the substrate. The Pt heater was heated up to 650°C. The sensor was placed in the exhaust line of a diesel-powered car engine and showed a response similar to that of commercial linear oxygen sensors used to control the combustion in automotive industry: good sensitivity to O<sub>2</sub> concentration ranging from 2 to 20%, response time of 5s and recovery time of 350s.

### C. STFO60 Deposition on the SOI Membrane

An STFO60 material similar to the one used in the experiment described above, provided by Innovative Materials, prepared as in [5], was acquired for the purpose of this study.

STFO60 powder was mixed with terpineol forming highly viscous slurry. Instead of alumina, we employed an SOI membrane as the substrate onto which STFO60 was deposited. Due to the reduced dimensions of the circular SOI micro-hotplate membrane (600 $\mu$ m diameter, 5 $\mu$ m thickness), the deposition of the sensing layer is a critical process. The slurry containing STFO60 is not suitable for ink-jet deposition; therefore a “dip-and-drop” technique has been adopted instead. Both a manual (using a micromanipulator) and an automatic (using NLP2000 from NanoInk) method have been employed to deposit the slurry on the membrane. The manual deposition was less accurate in terms of the amount of material deposited and the covered surface. After drying, an STFO60 layer of 3 to 5 $\mu$ m thickness was obtained (Fig. 5). The more accurate automatic deposition process led to an STFO60 layer of 1 $\mu$ m thickness (Fig. 6). From the point of view of the thermal stability of the whole structure, the latter value of the thickness value is more appropriate.

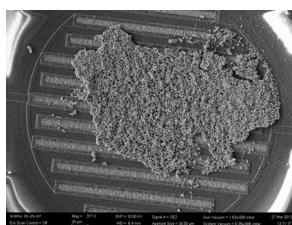


Fig. 5. SEM of the STFO layer manually deposited on the SOI membrane with Au IDEs.

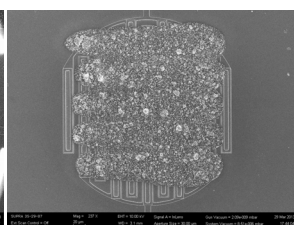


Fig. 6. SEM of the STFO layer mechanically deposited on the SOI membrane.

An annealing process was needed in order to stabilize the sensing layer. Two sets of tests were performed for an optimal temperature choice: thermo-gravimetric analysis (for the detection of the optimal firing temperature allowing removal of all organic components) and device resistance measurement while rising the temperature (for a stable electrical behavior). Fig. 7 presents the variation of the weight of STFO60 with temperature. The steep variation occurring at 200 $^{\circ}$ C is due to terpineol loss. Beyond 400 $^{\circ}$ C the material is stable from the chemical point of view.

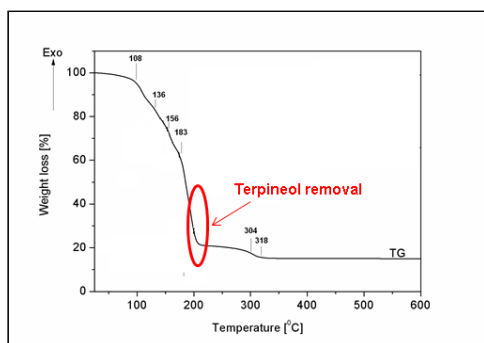


Fig.7. STFO60: thermo-gravimetric analysis.

But the temperature of about 400 $^{\circ}$ C is not enough to obtain a stable device from electrical point of view. More structural modifications take place above 400 $^{\circ}$ C without major changes in material density. In order to investigate the electrical behavior the device has been further heated using its own heater up to 800 $^{\circ}$ C. The heater temperature was kept constant at its maximum value for 5 minutes. During this “conditioning”

process, the sensing layer changed its color from black (at room temperature) to yellow-brown (at around 550 $^{\circ}$ C) and then again to black (above 700 $^{\circ}$ C). The electrical resistance of the layer has been monitored during conditioning and its behavior is shown in Fig. 8. The drop in resistance corresponds to color change from black to yellow-brown. The origins and temperature behavior of metal-insulator transition in perovskites are well documented [17]; it was demonstrated that STFO samples subject to a DC field stress exhibit a conductivity increase [18]. This is confirmed by our samples. As shown in Fig. 8, the resistance drops dramatically above 550 $^{\circ}$ C (Fig. 7).

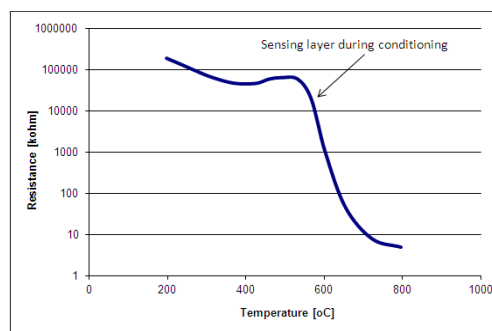


Fig. 8. Sensing layer resistance vs. temperature during annealing

The STFO60 layer proved to be highly porous and uniformly distributed on the IDEs, as shown in Fig. 9. This was mainly due to the fact that, during the conditioning process, the solvent and the binder inside the slurry were removed and the STFO60 particles got in close contact, thus yielding a continuous layer. The EDX analysis performed on the STFO60 layer, before and after conditioning (Fig. 10), shows the significant chemical process that the STFO60 undertook during the annealing process. Before conditioning, peaks corresponding to carbon and gold were present in the EDX. After annealing, the carbon and gold peaks completely disappeared, indicating removal of additional compounds in the sensing layer. Fe and Ti concentrations in the film are in good agreement with the envisioned STFO60 stoichiometry.

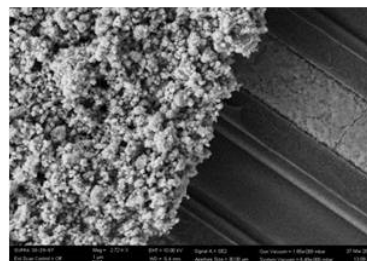


Fig. 9. SEM of the STFO layer after annealing.

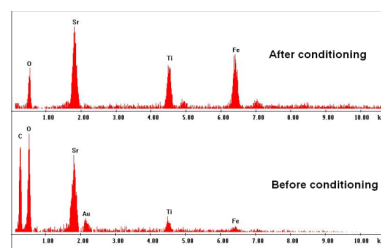


Fig. 10. EDX analysis on the STFO after and before conditioning.



### III. SENSOR PERFORMANCE

The STFO-SOI micro-hotplate resistive sensing structure was experimentally tested in an  $N_2$  atmosphere, where the  $O_2$  concentration was varied from 1% to 32%. The heater temperature was set at  $600^\circ C$ . The results in Fig. 11 show p-type behavior, good sensitivity and fast response. The response time was less than 6s, while the recovery time was less than 20s (with a fast recovery up to 90% in less than 7s). This is the first experimental test proving the feasibility of the STFO-SOI structure as  $O_2$  sensor. Further work needs to be devoted to reducing the thickness of the sensing layer below  $1\mu m$ . This will improve both the sensitivity and the response times of the sensor and will increase its reliability. The post-deposition annealing step ("conditioning") also needs to be optimized (both in terms of temperature range and time). Another problem is related to the time stability of this sensor. Drift is a well-known problem of the resistive gas sensors, therefore effort will be dedicated to understand its causes and build a reliable product.

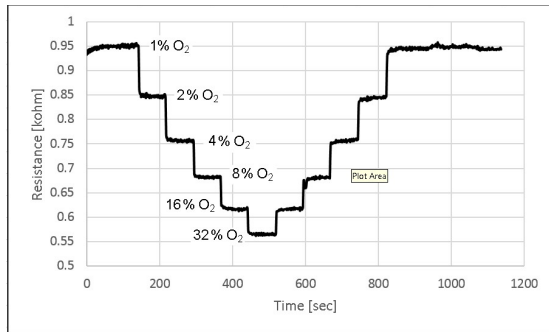


Fig. 11. SOI-based sensor response to oxygen, at room temperature. The heater temperature was set at  $600^\circ C$ .

### IV. CONCLUSIONS

A fully CMOS-compatible resistive oxygen sensor has been reported, comprising a SOI micro-hotplate membrane as substrate and STFO60 as sensing layer. A  $1\mu m$  thick STFO60 layer was deposited on a  $5\mu m$  thick SOI membrane and annealed at  $800^\circ C$ , for 5 minutes. Good sensitivity to  $O_2$  concentration from 1 to 32% and response time below 6s were measured at room temperature. The heater temperature was set at  $600^\circ C$ . This is the first experimental result showing the  $O_2$  sensing potential of this structure. Issues such as the deposition of a thinner sensing layer and long-time stability still need to be addressed in order to optimize the sensor. However, the use of a commercial, highly-mature CMOS process enables the fabrication of the sensing structure in high volume, at low cost. Owing to the already proven successful operation at high temperature of both STFO60 and SOI micro-hotplate, the sensing structure introduced in this paper has the potential to cope with harsh environment operation conditions.

### ACKNOWLEDGMENT

The authors would like to acknowledge the support of Dr. Adrian Dinescu and Dr. Mihai Danila at IMT-Bucharest, Prof. Giacomo Cao at Innovative Materials SRL and Dr. Robert Stokes at NANOINK Inc.

### REFERENCES

- [1] M. Quaranta, S.M. Borisov, I. Klimant, "Indicators for optical oxygen sensors", *Bioanal Rev*, vol. 4, pp. 115–157, 2012.
- [2] A. Quoc Pham, R. S Glassal, "Novel Oxygen pumping characteristics of yttria-stabilized-zirconia", *Electrochimica Acta*, vol. 43 (18), pp. 2699–2708, 1998.
- [3] C. Lopez-Gandara, F.M. Ramos, A. Cirera, "YSZ-Based Oxygen Sensors and the Use of Nanomaterials: A Review from Classical Models to Current Trends", *Journal of Sensors*, vol. 2009, ID 258489, 2009.
- [4] P. K. Guha et al., "Novel design and characterization of SOI CMOS micro-hotplates for high temperature gas sensors", *Sensors and Actuators B: Chemical*, vol. B 127, pp. 260–266, 2007.
- [5] G. Neri et al., "FeSrTiO<sub>3</sub>-based resistive oxygen sensors for application in diesel engines", *Sensors and Actuators B: Chemical*, vol. B 134, pp. 647–653, 2008.
- [6] S. Maeng et al., "SOI CMOS-based smart gas sensor system for ubiquitous sensor networks", *ETRI Journal*, vol. 30, pp. 516–525, 2008.
- [7] S. Santra et al., "ZnO nanowires grown on SOI CMOS substrate for ethanol sensing", *Sensors and Actuators B: Chemical*, vol. 146, pp. 559–565, 2010.
- [8] S. Z. Ali et al., "Nanowire hydrogen gas sensor employing CMOS micro-hotplate", *Proceedings of the 8<sup>th</sup> IEEE Sensors Conference*, pp. 114–117, 2009.
- [9] S. Santra, P. Guha, S. Ray, F. Udrea, J. Gardner, "SOI CMOS integrated zinc oxide nanowire for toluene detection", *Proceedings of the 5<sup>th</sup> International Nanoelectronics Conference (INEC)*, pp. 119–121, 2013.
- [10] F. Udrea et al., "Three technologies for a smart miniaturized gas-sensor: SOI CMOS, micromachining, and CNTs-challenges and performance", *Proceedings of the International Electron Devices Meeting, (IEDM) 2007*, pp. 831–834, 2007.
- [11] S. Santra et al., "Post-CMOS wafer level growth of carbon nanotubes for low-cost microsensors—a proof of concept," *Nanotechnology*, vol. 21, pp. 485301, 2010.
- [12] J. W. Gardner, T. Ahmed, P. Moseley, S. Ali, M. Chowdhury, and F. Udrea, "High temperature robust SOI ethanol sensor," *Procedia Engineering*, vol. 25, pp. 1317–1320, 2011.
- [13] S.Z. Ali et al., "A High Temperature SOI CMOS NO Sensor," *AIP Conference Proceedings*, 1362, pp. 53–54, 2011.
- [14] R. Moos, W. Menesklou, H.-J. Schreiner, K.H. Hardtl, "Materials for temperature independent resistive oxygen sensors for combustion exhaust control", *Sensors and Actuators B: Chemical*, vol. B 67, pp. 178–183, 2000.
- [15] A. Rothschild et al., "Temperature independent resistive oxygen sensor based on SrTi<sub>1-x</sub>Fe<sub>x</sub>O<sub>3-δ</sub> solid solutions", *Sensors and Actuators B: Chemical*, vol. B 108, pp. 223–230, 2005.
- [16] G. Neri et al., "Resistive  $\lambda$ -sensors based on ball milled Fe-doped SrTiO<sub>3</sub> nanopowders obtained by self-propagating high-temperature synthesis (SHS)", *Sensors and Actuators B: Chemical*, vol. B 126, pp. 258–265, 2007.
- [17] K. Szot, W. Speier, W. Eberhardt, "Switching the electrical resistance of individual dislocations in single-crystalline SrTiO<sub>3</sub>", *Applied Physics Letters* 60(10), pp. 1190–1192, 1992.
- [18] M. Wojtyniak et al., "Electro-degradation and resistive switching of Fe-doped SrTiO<sub>3</sub> single crystal", *Journal of Applied Physics*, Vol. 113, 083713, 2013.